Supplementary of

Significant influence of oxygenated volatile organic compounds on atmospheric chemistry analysis: A case study in a typical industrial city in China

Jingwen Dai et al.

Correspondence: Li Li (Lily@shu.edu.cn) and Kun Zhang (zk1231@shu.edu.cn)

Text S1 Adjustments of model parameter

The base parameter settings of the OBM were shown in Sec 2.2. As formal studies have reported, PKU-Mo as a catalytic converter for NO_2 measurement can cause interferences from other nitrogen–oxygen compounds (e.g., PAN, HNO_3), which can lead to an overestimation NO_2 by 30%~50% (Kim et al., 2015; Tan et al., 2017, 2019; Xu et al., 2013). In addition, strong anthropogenic emissions (such as vehicle emissions) around these sites, the model might not be able to reach the steady state resulting in positive deviation (Li et al., 2014). Therefore, the observed NO_2 concentrations among those 5 sites were reduced by 30%~40% to compensate for interferences from catalytic converter (Xu et al., 2013), and NO steady-state approximations (NOss) was calculated (Del Negro et al., 1999), which were then used for OBM inputs. Simulation constrained by all observed parameters including OVOCs and adjusted NO_2 and NO serves as the Base scenario. In order to investigate the impacts of model with OVOCs observationally constrained, scenario Free (Table S3) was conducted on top of the Base scenario by excluding observation constraints of OVOCs so that they were mainly generated by the oxidation of precursor VOCs in OBM.

Text S2 Model validation

The time series plot of modeled and observed O_3 (Figure S6) and the model validation parameters were shown in (Table S4). The box model could be able to capture the diurnal variations of O_3, but the scenario M0 generally overestimated the O_3 peaks, which may be related to the overestimation of NO_2. After adjusting for the observed NO_2 concentrations by cutting by 30%~40% (40% for ZL, CQ and XD, 30% for CD and TZ) in scenario M1, the peak of O_3 in M1 was significantly decreased. It showed that the observed NO concentrations were significantly higher than the modeled NO in scenario M0 and M1. As discussed before, there was strong vehicle emissions nearby those sites especially during August 8-9, which may result in failing to reach steady stat. By further adjusting the input of NO to the approximate steady state concentration (NOss) in scenario M2 for each site, the peak of O_3 was further reduced that counteracted the reduction of titration of O_3 by NO, and closer to the observations overall (Figure S6 (b)). The modeled O_3 remain underestimate or overestimate at some times during the daytime, and significantly underestimate at night (Figure S11). This discrepancy may be due to the limitations of the 0-D model to express the transport processes in the atmosphere due to its simplification of atmospheric physical processes. The simplification of physical process is acceptable for modeling of in situ photochemistry.

Text S3 Simulations of OVOCs in the Free scenario

Similar to Base scenario but without OVOCs observationally constraints in the Free scenario, the hourly average concentration of OVOCs at five sites was 24.7±7.2 ppb, with a 59.1% overpredict of observations (15.5±11.3 ppb). OVOCs at CD (18.7±4.1 ppb), CQ (26.3±6.6 ppb), XD (24.7±7.0 ppb), and ZL (32.1±6.2 ppb) sites were overestimated in Free scenario by 81.4%, 88.4%, 42.1%, and 126.5%, respectively. The OVOCs concentrations in the atmosphere are subject to a combination of emission, secondary generation, and removal processes. Given that direct emissions of OVOCs are not considered in the Free scenario, the OVOCs concentrations in the model are determined by the generation and removal processes. In terms of the production process, it can be influenced by the emission of precursor VOCs indirectly. It has shown that in the presence of strong emission sources of VOCs, the model might not be able to reach an steady state, leading to a significant overestimation (Li et al., 2014). The observed OVOCs at TZ during August 8 were unusually high due to transient emissions (Figure S6 (c)), pulling up the average levels. However, during the later days, the modeled OVOCs (15.5±10.7 ppb) were also higher (15.3%) than the observed concentrations (13.4±11.5 ppb) consisting with the other sites.

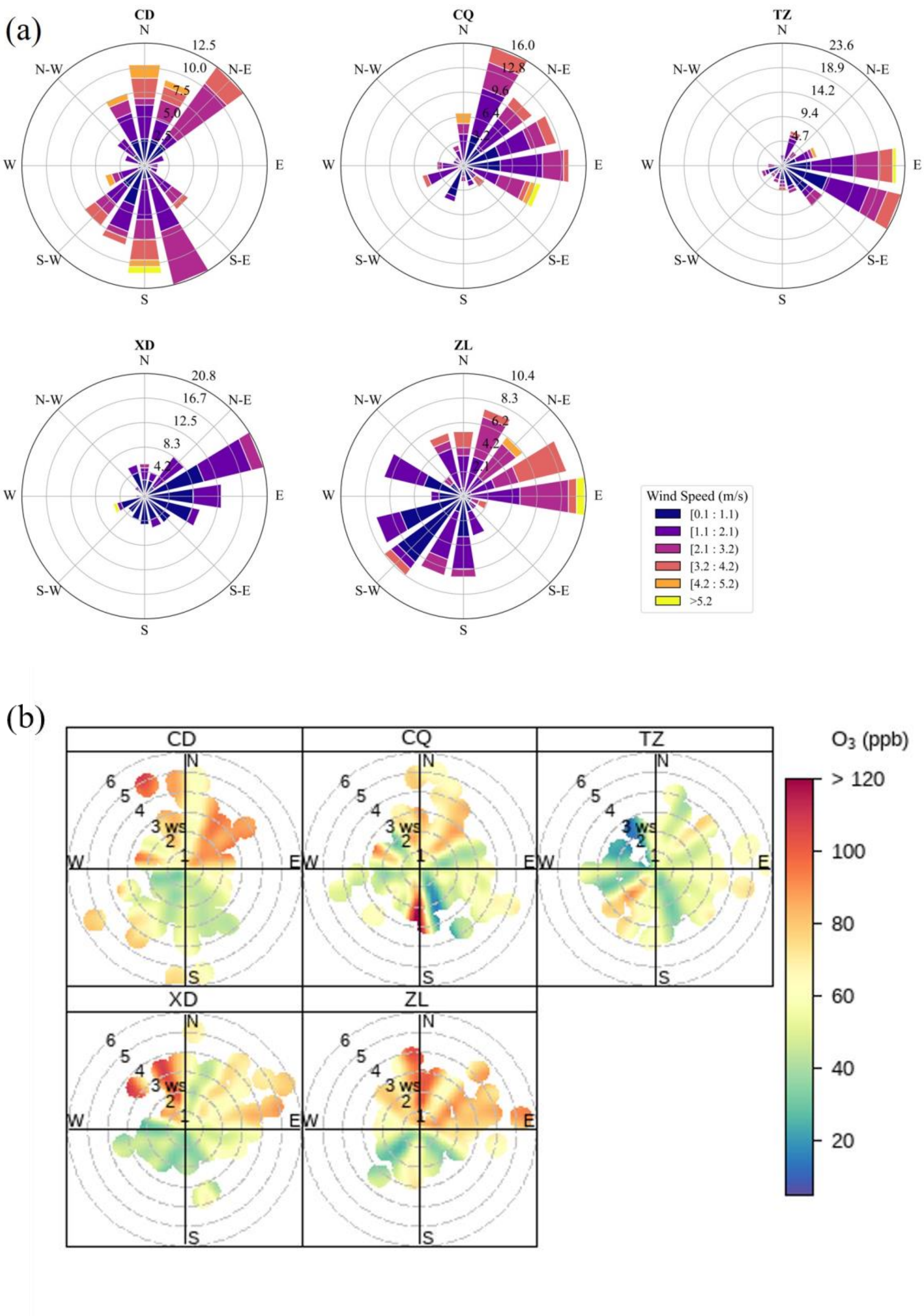

Figure S1 (a) Wind rose and (b) O_3 pollution rose diagram of each site during the observation period.

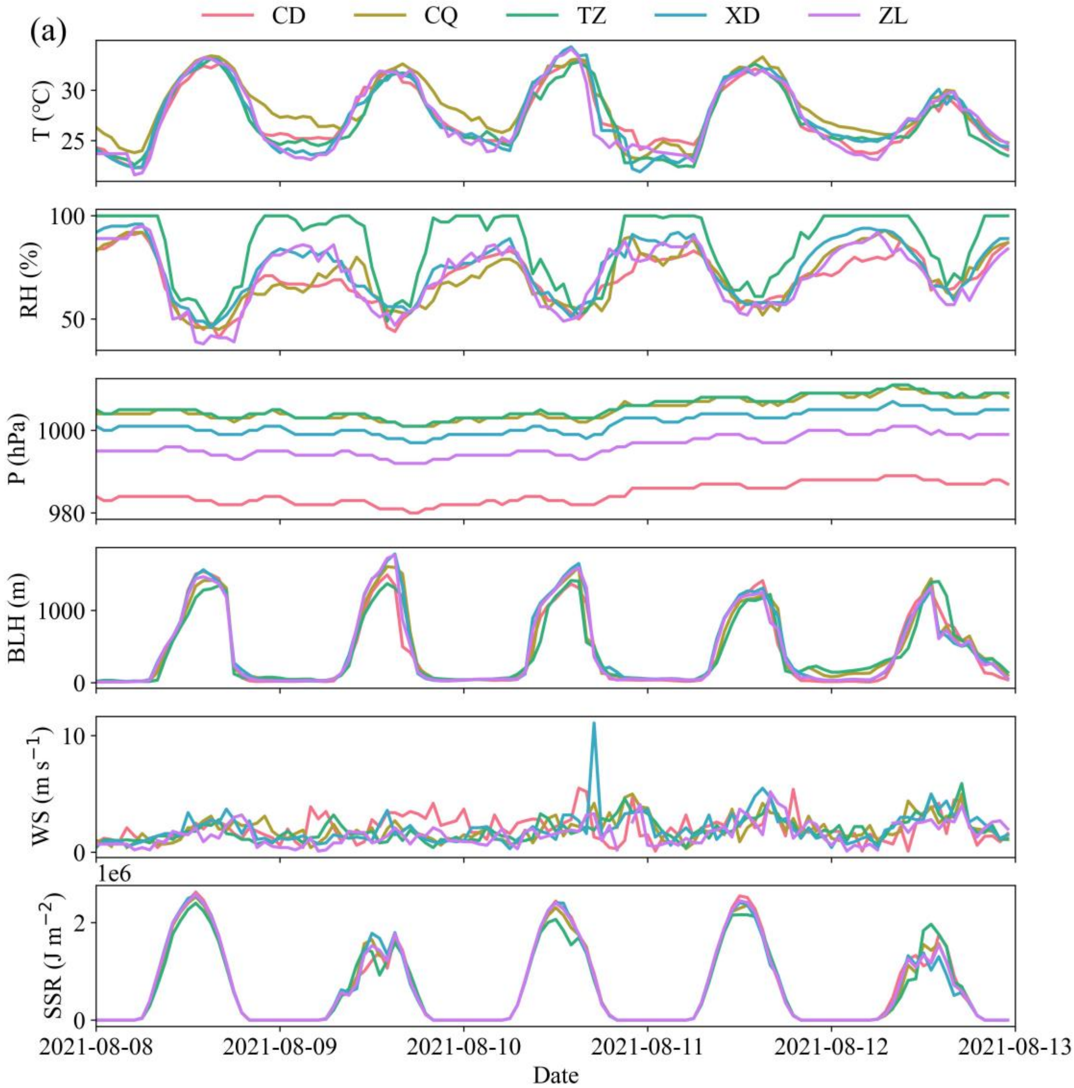
(a)
CD
CQ
TZ
XD
ZL
T (°C)
30
25
RH (%)
100
50
P (hPa)
1000
980
BLH (m)
1000
0
WS (m s^{-1})
10
0
1e6
SSR (J m^{-2})
2
0
2021-08-08
2021-08-09
2021-08-10
2021-08-11
2021-08-12
2021-08-13
Date

56

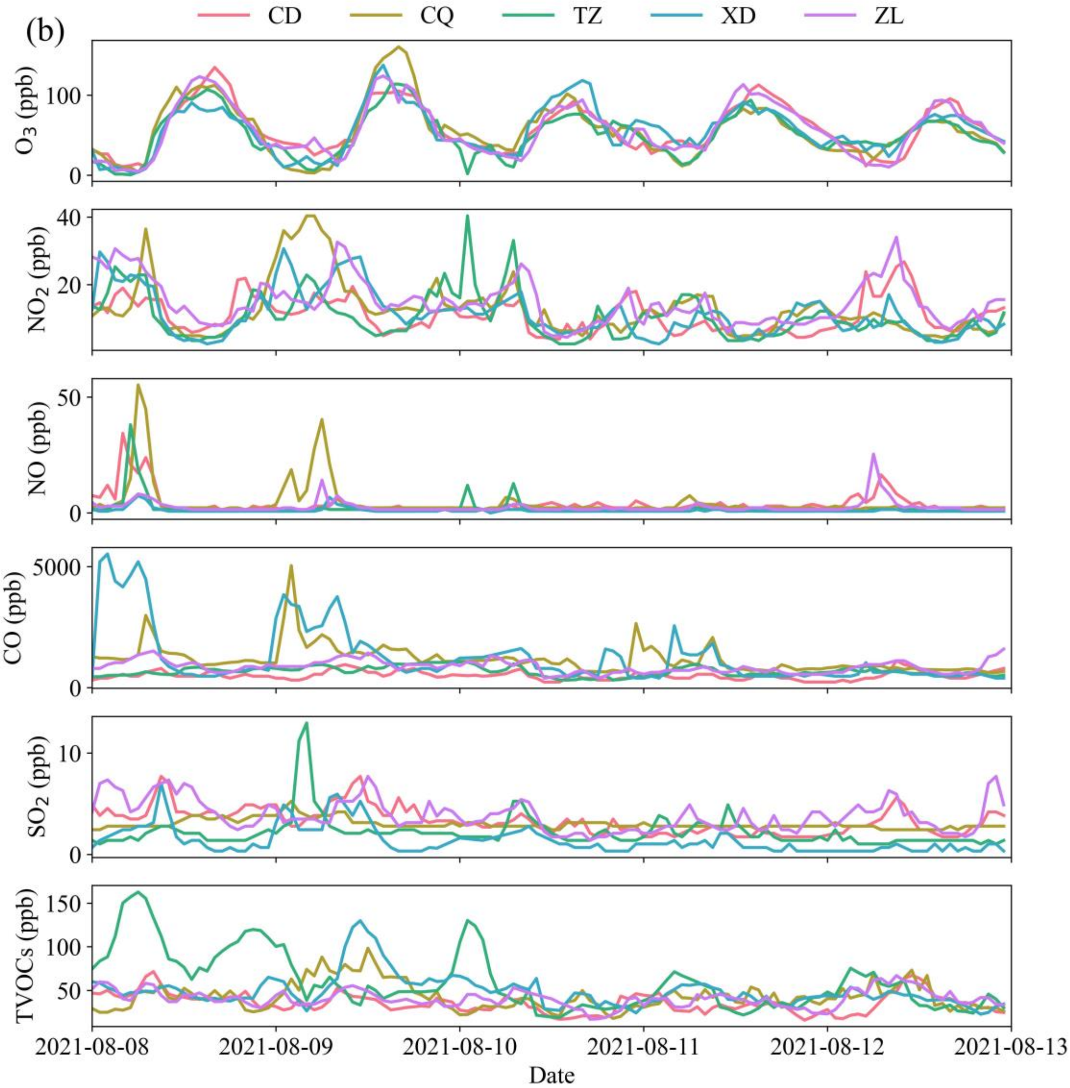

Figure S2 Time series of (a) meteorological parameters and (b) major pollutant mixing ratios at five sites in Zibo.

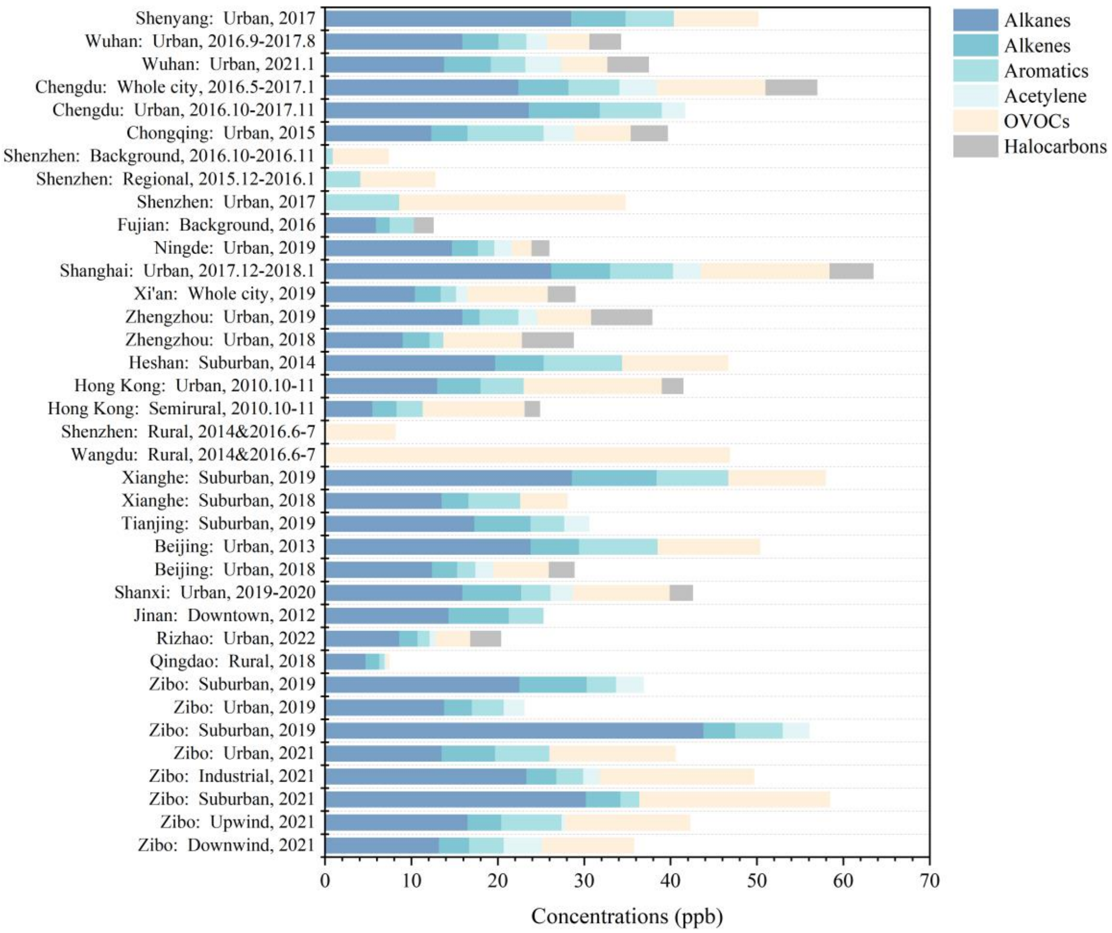

Figure S3 Comparison of VOC concentrations and compositions in this study with former studies based on Table S4.

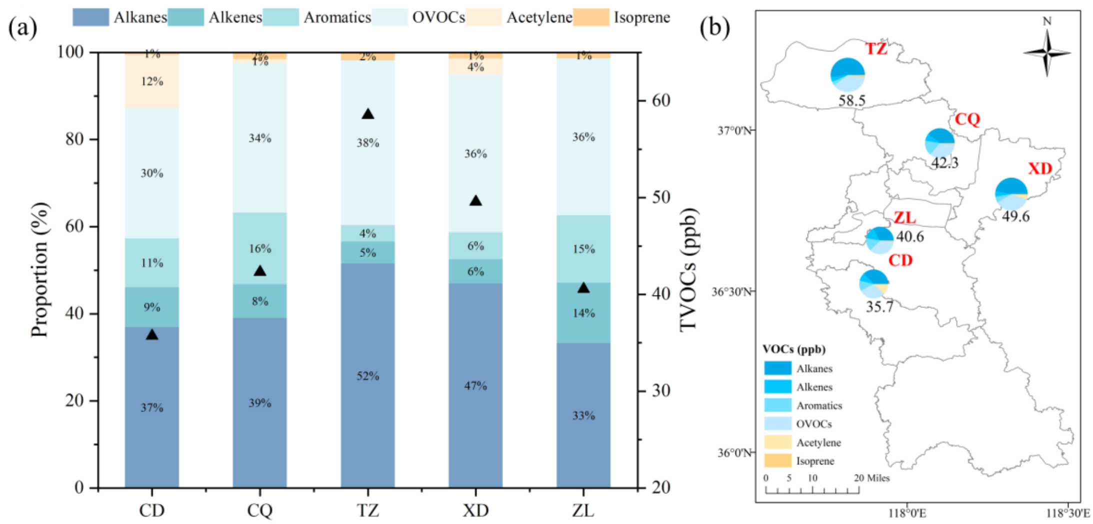

Figure S4 (a) Comparison and (b) spatial distribution of VOCs components among five sites.

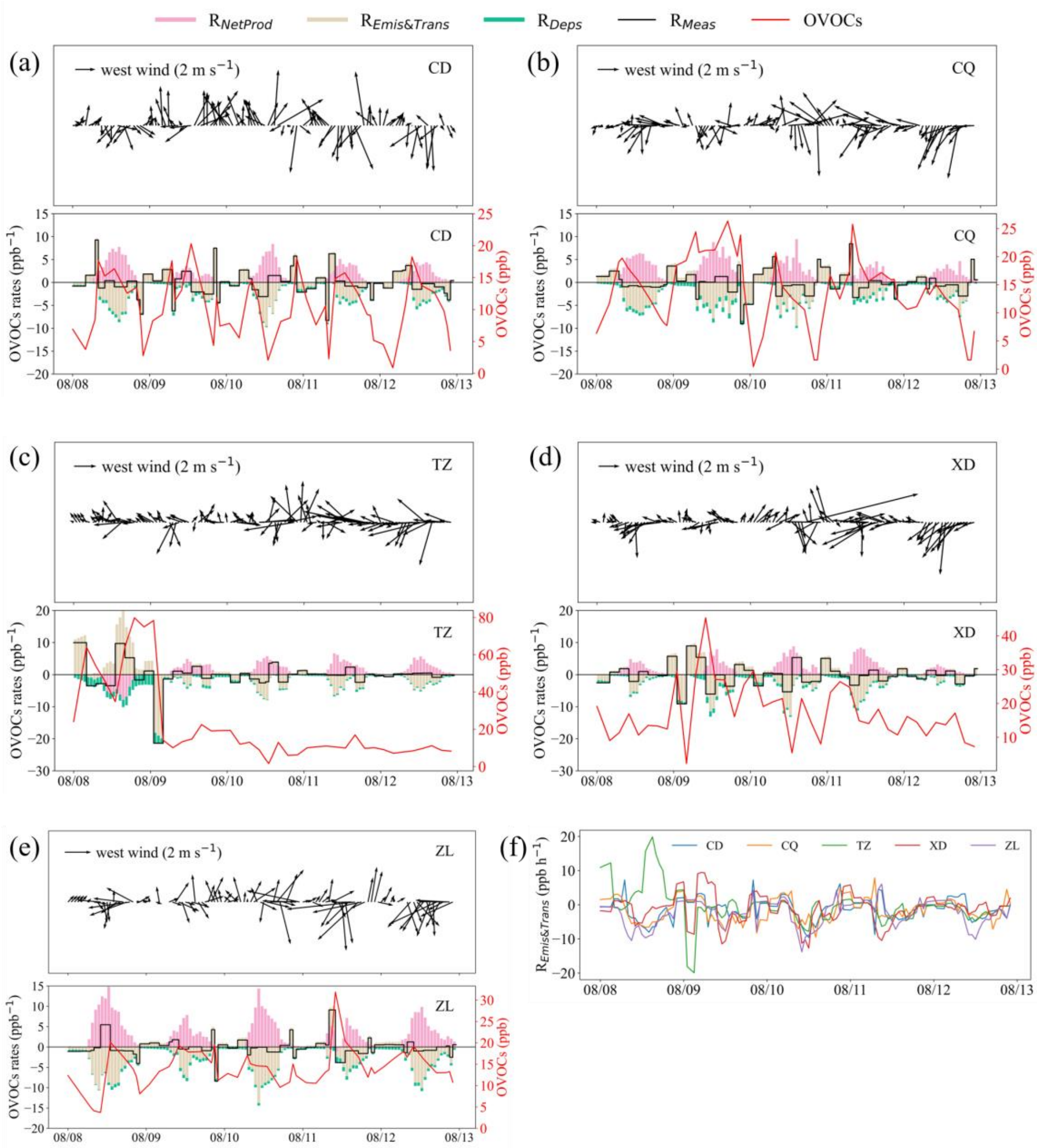

Figure S5 OVOCs accumulation and contributions from local net photochemical production and emissions/transport, and winds at (a) CD, (b) CQ, (c) TZ, (d) XD, and (e) ZL sites, respectively, and (f) time variations of $R_{Emis\&Trans}$ for all sites. $R_{NetProd}$, $R_{Emis\&Trans}$, R_{Dep} and R_{Meas} in the legend represent local net O3 photochemical production, emissions and regional transport, deposition and observed OVOCs formation rates, respectively.

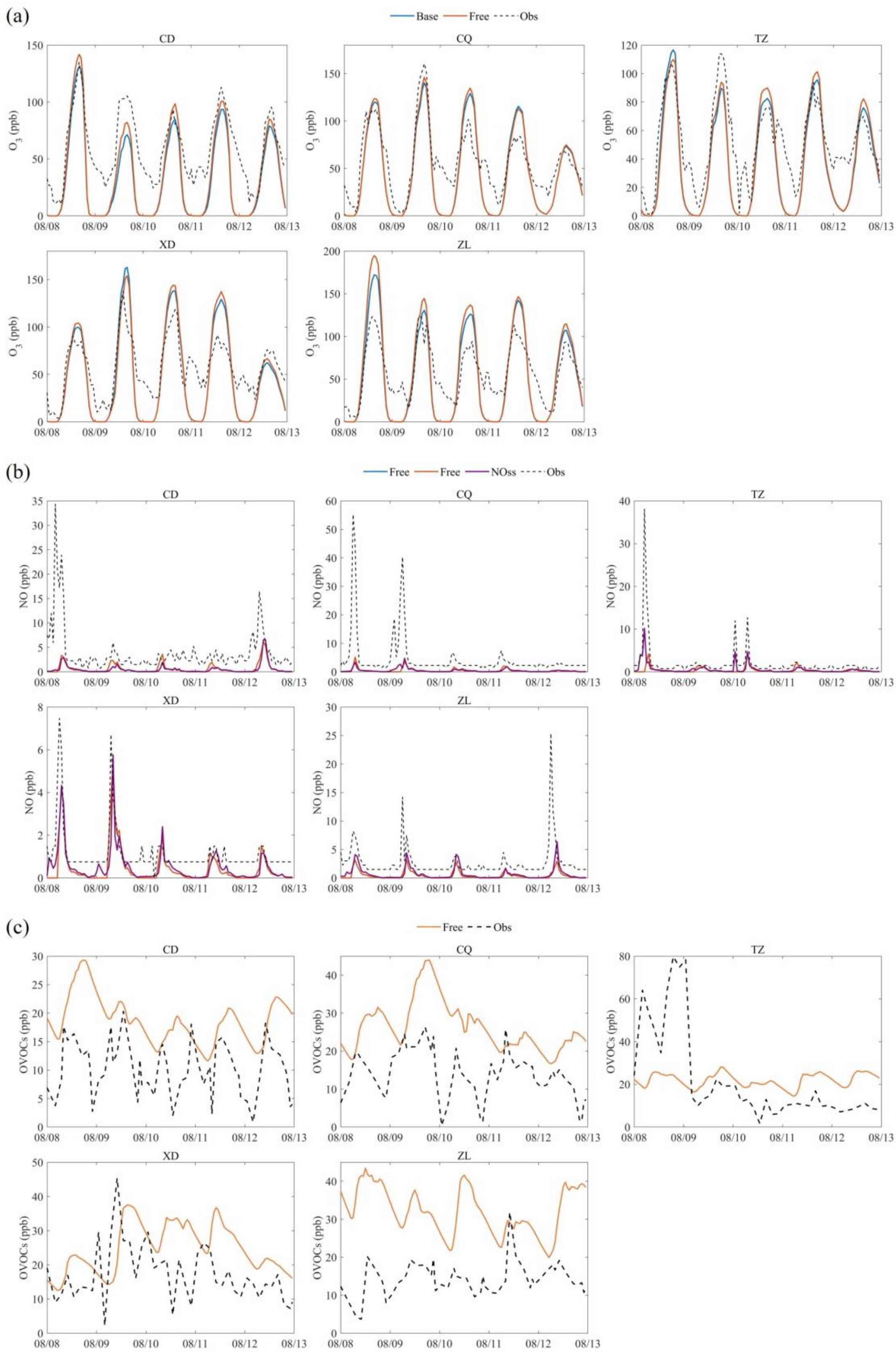

Figure S6 Time series of O_3, NO_x from observations (Obs), simulations (Base and Free scenarios) and NO steady state (NOss), and that of OVOCs only including input species from observation and Free scenario.

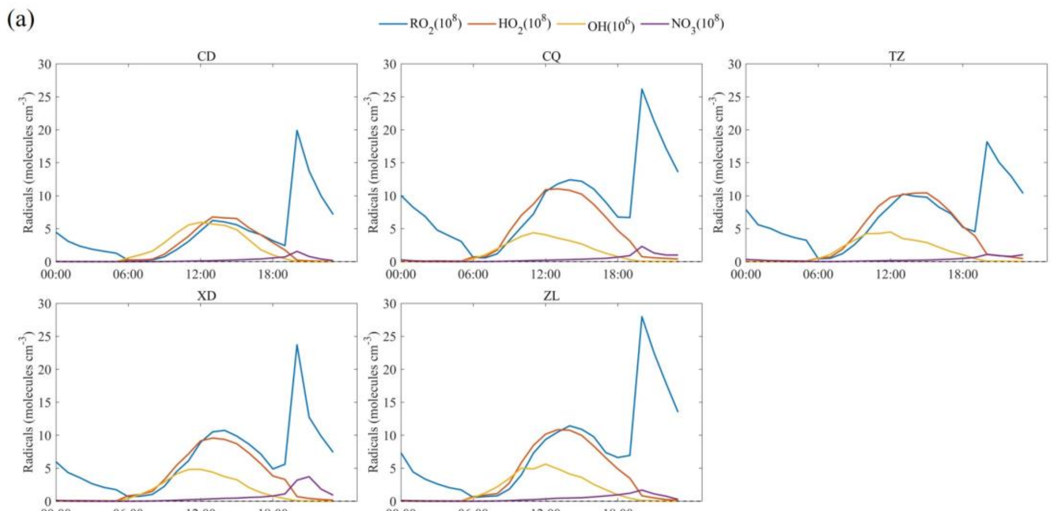

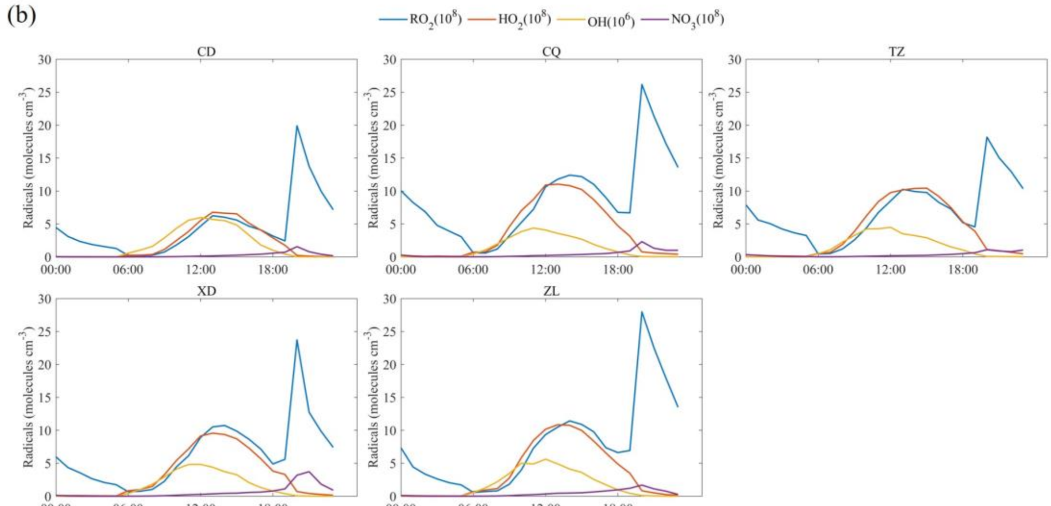

Figure S7 (a) Simulated average daytime variation of RO*x* (RO_2, HO_2, and OH) and NO_3 radicals at five sites, and (b) the effects of OVOCs observationally constrains on radical concentrations, calculated by (Free – Base).

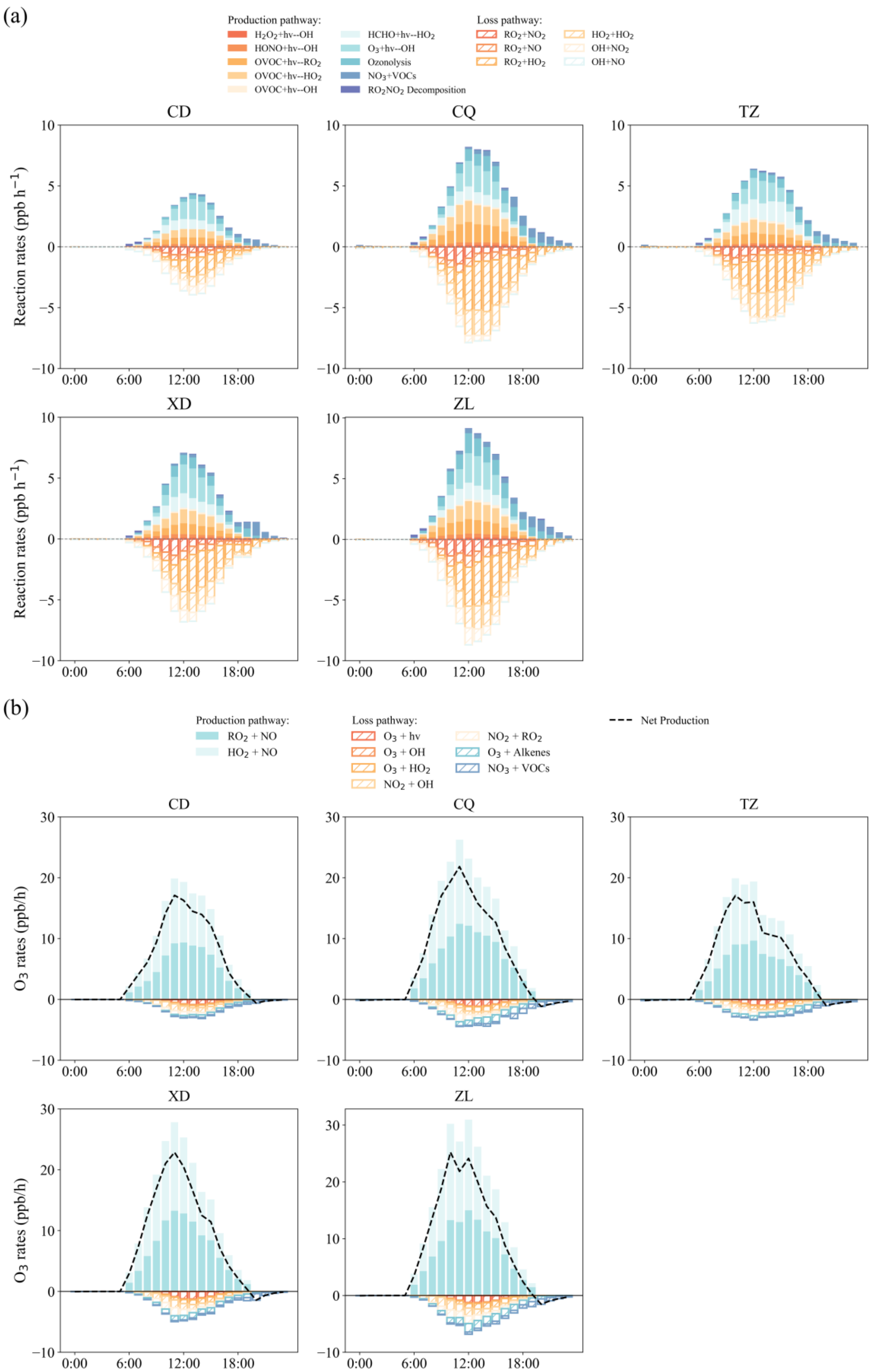

Figure S8 Average diurnal profiles of sources and sinks of (a) RO_x and (b) O_3 in the Base scenario.

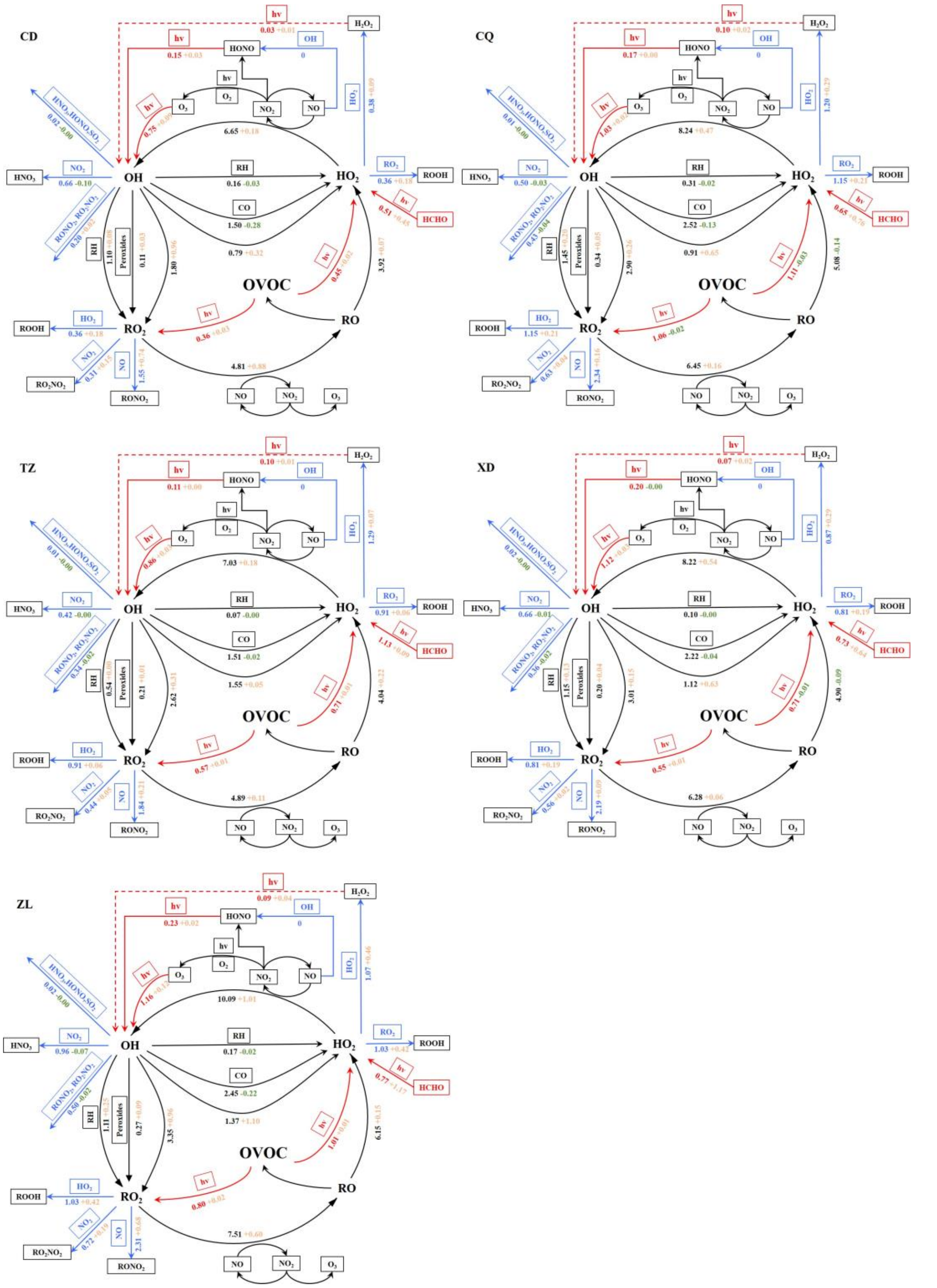

Figure S9 Daytime (8:00-18:00 LT) average budgets of RO_x radicals (in ppb h^{-1}) at each site in Base scenario and the difference between Free and Base scenario. The first values were the rates of Base, followed by the difference between Free and Base, where '-' means that the rate of Free scenario is lower than that of Base (in green), and conversely '+' means that the rate of Free is higher than that of Base (in orange). Primary RO_x sources and sinks are in red and blue, respectively, and the black lines represent the processes in RO_x and NO_x recycling.

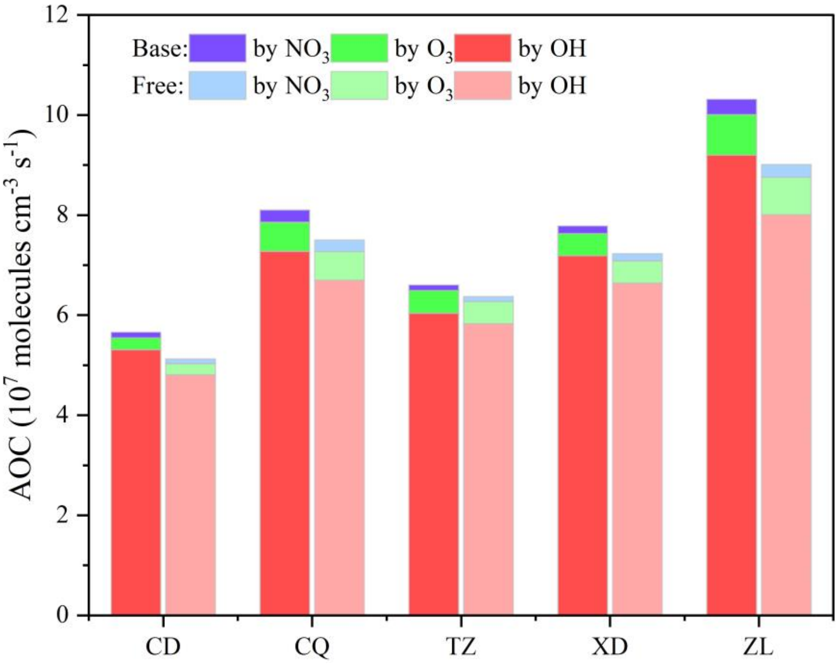

Figure S10 Comparison of daytime atmospheric oxidation capacity (AOC) between Base and Free scenario.

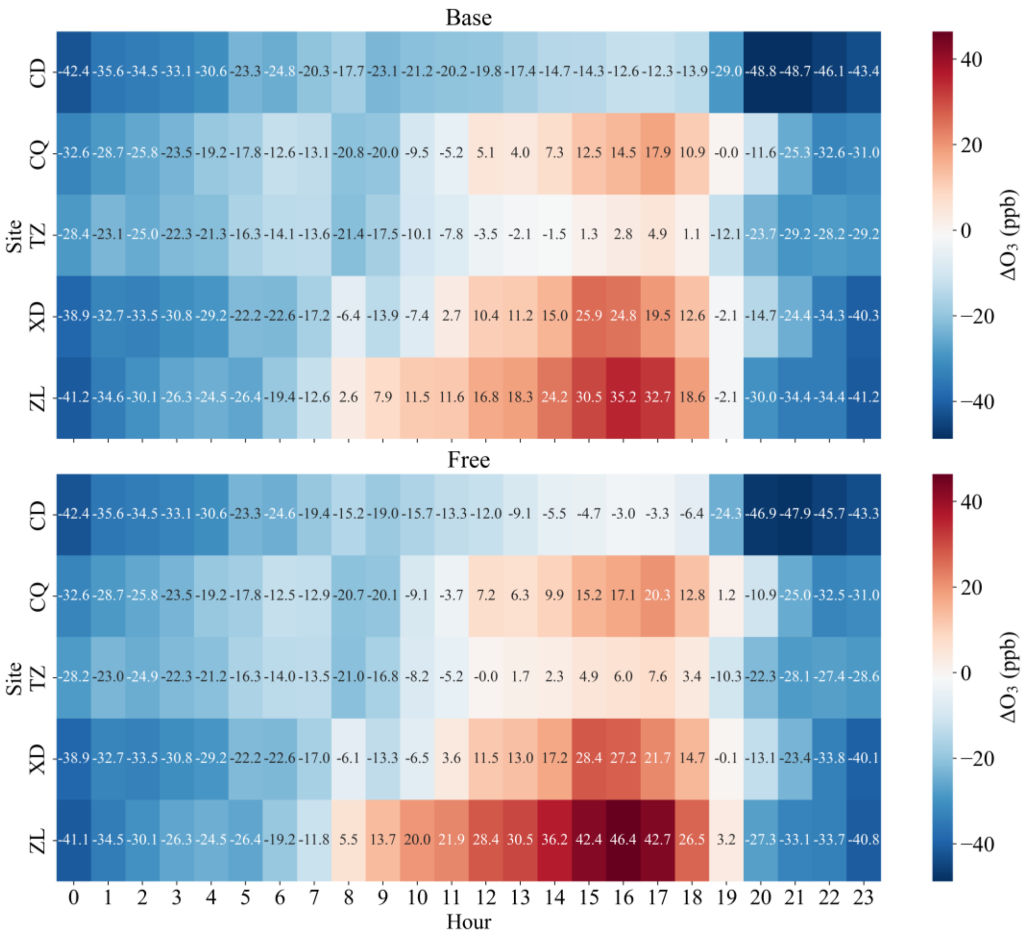

Figure S11 Heat map of O_3 concentration difference (ΔO_3 = Sim - Obs) between simulated and observed of Base and Free scenario

Table S1 Location and site classification for the five different sites of Zibo

Site name	Site	Longitude	Latitude	Style	Meteorological sites
Chengdong	CD	117°53'E	36°31'N	Downwind	Boshan
Chengqu	CQ	118°60'E	36°57'N	Upwind	Huantai
Tianzhen	TZ	117°48'E	37°10'N	Suburban	Gaoqing
Xindian	XD	118°19'E	36°48'N	Industrial	Linzi
Zhonglou	ZL	117°54'E	36°39'N	Urban	Zichuan

Table S2 Comparison of VOC concentrations and compositions in this study with former studies.

City	Site	Type	Period	Species	TVOCs	Alkanes	Alkenes	Aromatics	Acetylene	OVOCs	Halocarbons	References
Zibo	CD	Downwind	August 8-13, 2021	74	35.3	13.4	3.4	4.1	4.0	10.4		This study
	CQ	Upwind			42.6	16.9	3.9	7.5	0.5	13.9		
	TZ	Suburban			55.1	29.4	3.8	2.1	0.0	19.7		
	XD	Industrial			47.0	22.3	3.4	2.9	1.6	16.8		
	ZL	Urban			41.3	14.3	5.8	6.2	0.0	14.9		
	TZ	Suburban	High-O_3 episodes in July 2019	56	58.1	43.8	3.7	5.5	3.1			(Li et al., 2021)
	BJ	Urban			23.8	13.8	3.2	3.7	2.4			
	XD	Suburban			38.1	22.5	7.8	3.4	3.2			
Qingdao		Rural	October 5 to November 10, 2018	106	7.6	4.7	1.6	0.6	0.2	0.4		(Liu et al., 2021a)
Rizhao		Urban	December 2021 to October 2022	111	19.7	8.6	2.1	1.4	0.7	4.0	3.6	(Zhang et al., 2023)
Jinan		Downtown	June 2010 to May 2012	55	25.3	14.3	7.0	4.0				(Wang et al., 2016)
Shanxi	LL	Urban	2019-2020	115	44.4	19.4	5.3	4.5	1.8	10.8	2.7	(Liu et al., 2023)
	LF				45.7	14.3	9.1	3.2	2.9	13.2	2.6	
	YC				37.5	13.9	5.9	2.4	3.1	9.6	2.7	
Beijing		Urban	2018	99	29.1	12.4	2.9	2.1	2.1	6.4	3.0	(Li et al., 2022)
Tianjing		Suburban	November 1, 2018 to March 15, 2019	54	30.6	17.3	6.5	3.9	2.9			(Gu et al., 2020)
Xianghe		Suburban	August 7-25, 2018	65	28.1	13.5	3.1	6.0		5.5		(Yang et al., 2021)
			December 1, 2018 to January 5, 2019		58.0	28.6	9.8	8.3		11.3		

City	Site	Type	Period	Species	TVOCs	Alkanes	Alkenes	Aromatics	Acetylene	OVOCs	Halocarbons	References
Wangdu	WD	Rural	2014 and 2016(June–July)	17	52.4					46.9		(Han et al., 2019)
Shenzhen	YMK	Rural			11.1					8.2		
Heshan		Suburban	October 20 to November 22, 2014	56	46.6	19.7	5.6	9.1		12.3		(Yang et al., 2017)
Beijing		Urban	August 10-27, 2013		50.4	23.8	5.6	9.1		11.9		
Zhengzhou		Urban	May 3-24, 2018	103	29.1	9.0	3.1	1.6		9.1	6.0	(Li et al., 2020)
Zhengzhou		Urban	July 2019	106	38.6	15.9	2.0	4.5	2.2	6.2	7.1	(Wang et al., 2022)
Xi'an		Whole city	June 20 to July 20, 2019	99	29.1	10.4	3.0	1.8	1.3	9.3	3.2	(Song et al., 2021)
Shanghai		Urban	2017.12.5-2018.1.15	113	63.6	26.2	6.8	7.3	3.2	14.9	5.1	(Liu et al., 2021b)
Ningde		Urban	March-May, 2019	94	25.0	15.0	3.0	1.6	2.0	1.7	1.7	(Chen et al., 2024)
			June-August, 2019		20.0	9.5	2.6	1.5	1.4	3.0	1.9	
			September-November, 2019		22.4	12.2	2.3	1.9	1.4	2.1	2.5	
			January-February, 2019		36.5	22.3	4.1	2.5	3.1	2.3	2.1	
Fujian	Mt. Wuyi	Background	August-October 2016	70	6.1	1.9	1.1	1.3			1.8	(Hong et al., 2019)
	XM	Urban		70	17.9	9.1	2.1	4.1			2.6	
	FZ	Urban		70	14.1	6.8	1.7	3.1			2.5	
Shenzhen	SZ-U	Urban	December 2017	18	35.7			8.6		26.2		(Huang et al., 2019)
	NA-R	Regional	December 20, 2015 to January 15, 2016		13.5			4.1		8.7		
	NL-B	Background	October 31, 2016 to November 14, 2016		8.2			0.9		6.5		

City	Site	Type	Period	Species	TVOCs	Alkanes	Alkenes	Aromatics	Acetylene	OVOCs	Halocarbons	References
Chongqing	JYS	Urban	August-September 2015	96	23.0	6.1	1.4	16.1	1.8	6.8	4.9	(Li et al., 2018)
	CJZ	Urban		96	49.9	17.7	7.1	5.8	5.2	7.6	4.8	
	NQ	Urban		96	34.1	12.9	4.1	4.6	3.8	5.1	3.1	
Chengdu		Urban	Octorber 2016 to September 2017	55	41.8	23.6	8.2	7.2	2.7			(Song et al., 2018)
Chengdu		Whole city	May 2016 to January 2017	99	57.5	22.4	5.8	5.9	4.3	12.6	6.0	(Simayi et al., 2020)
Wuhan		Urban	Jan-21	106	37.4	13.8	5.4	4.0	4.2	5.3	4.8	(Xu et al., 2023)
Wuhan		Urban	September 2016 to August 2017	102	34.7	15.9	4.2	3.2	2.4	4.9	3.7	(Hui et al., 2018)
Shenyang		Urban	August 20 to September 16, 2017	58	40.4	28.5	6.3	5.6		9.8		(Ma et al., 2019)

Table S3 Summary of main meteorological parameters and average levels of pollutants during the observation period.

Parameter	CD	CQ	TZ	XD	ZL
WS (m s^{-1})	2.1±1.2	2.0±1.0	1.9±1.0	1.9±1.1	1.5±1.0
T (℃)	27.3±2.9	28.2±2.9	27.1±3.1	27.4±3.3	27.3±3.4
RH (%)	69.1±11.8	70.4±13.1	85.4±17	74.6±13.9	70.9±14.9
P (hPa)	984.6±2.5	1005.2±2.6	1005.6±2.6	1001.6±2.6	996.1±2.5
BLH (m)	421.2±512.2	451.5±510.1	421.3±465.1	463.9±541.2	443.8±528.3
SSR (10^5 J m^{-2})	6.7±8.3	6.5±8.1	6.3±7.7	6.6±8.2	6.6±8.2
NO (ppb)	3.9±4.7	4.5±7.8	1.9±4.1	1.1±1.1	2.6±2.9
NO_2 (ppb)	10.8±5.1	12.7±8.1	10.4±6.7	11.4±6.7	14.8±6.6
SO_2 (ppb)	3.4±1.3	3.0±0.5	2.2±1.6	1.4±1.3	3.9±1.5
CO (ppb)	508±173.6	1176.4±578.4	674.3±190.9	1261.4±1174.1	868±258.3
O_3 (ppb)	58.6±30.0	56.4±34.2	51.0±27.8	56.1±29.4	57.4±32.2
TVOCs (ppb)	35.7±12.5	42.3±15.4	58.5±35.0	49.6±19.0	40.6±10.3
Alkanes (ppb)	13.2±6.2	16.5±8.5	30.2±21	23.3±11.2	13.5±5.6
Alkenes (ppb)	3.3±1.8	3.3±1.6	2.9±1.7	2.8±1.3	5.6±3.0
Aromatics (ppb)	4.0±1.7	7±3.6	2.2±1.2	3.1±1.5	6.3±4.7
OVOCs (ppb)	10.7±5	14.5±6.7	22.1±22.5	17.9±8.5	14.6±4.8
Isoprene (ppb)	0.2±0.2	0.6±0.6	1.1±0.8	0.7±0.5	0.6±0.7
Alkyne (ppb)	4.4±4.1	0.4±0.7	0±0	1.9±1.6	0±0

Table S4 Modeled O_3 assessment of Base and Free scenario.

Site	Base		Free	
	IOA	R	IOA	R
CD	0.80	0.88	0.90	0.88
CQ	0.90	0.87	0.86	0.87
TZ	0.88	0.88	0.85	0.88
XD	0.86	0.88	0.83	0.89
ZL	0.88	0.89	0.88	0.87

Table S5 Comparison concentrations of the Base and Free scenario modeling parameters, including OVOCs, O_3, RO_2, HO_2, and OH) at the five sites.

Parameter	site	Conc		Parameter	site	Conc	
		Base	Free			Base	Free
OVOCs	CD	10.32	18.72	Daytime OH	CD	3.87E+06	3.06E+06
	CQ	13.98	26.33		CQ	2.78E+06	2.64E+06
	TZ	21.93	21.9		TZ	2.99E+06	2.94E+06
	XD	17.35	24.65		XD	3.10E+06	3.01E+06
	ZL	14.17	32.09		ZL	3.56E+06	3.20E+06
Daytime O_3	CD	60.89	68.17	Daytime HO_2	CD	4.13E+08	4.67E+08
	CQ	82.43	84.11		CQ	7.75E+08	8.58E+08
	TZ	66.18	68.76		TZ	7.56E+08	7.96E+08
	XD	85.16	86.71		XD	6.45E+08	7.34E+08
	ZL	96.77	106.26		ZL	7.26E+08	8.74E+08
Daytime $\|\Delta O_3\|$	CD	18.13	14.64	Daytime RO_2	CD	3.67E+08	4.96E+08
	CQ	18.03	18.13		CQ	8.25E+08	8.79E+08
	TZ	12.31	13.08		TZ	6.74E+08	7.29E+08
	XD	18.63	19.83		XD	6.79E+08	7.26E+08
	ZL	21.02	29.06		ZL	7.26E+08	8.72E+08

Note: Concentrations of OVOCs and O_3 in ppb, RO_2, HO_2 and OH in molecules cm^{-3}.; $|\Delta O_3|$ = |Sim – Obs|.

Reference

Chen, G., Liu, T., Chen, J., Xu, L., Hu, B., Yang, C., Fan, X., Li, M., Hong, Y., Ji, X., Chen, J., and Zhang, F.: Atmospheric oxidation capacity and O_3 formation in a coastal city of southeast China: Results from simulation based on four-season observation, J. Environ. Sci., 136, 68–80, https://doi.org/10.1016/j.jes.2022.11.015, 2024.

Del Negro, L. A., Fahey, D. W., Gao, R. S., Donnelly, S. G., Keim, E. R., Neuman, J. A., Cohen, R. C., Perkins, K. K., Koch, L. C., Salawitch, R. J., Lloyd, S. A., Proffitt, M. H., Margitan, J. J., Stimpfle, R. M., Bonne, G. P., Voss, P. B., Wennberg, P. O., McElroy, C. T., Swartz, W. H., Kusterer, T. L., Anderson, D. E., Lait, L. R., and Bui, T. P.: Comparison of modeled and observed values of NO_2 and JNO_2 during the Photochemistry of Ozone Loss in the Arctic Region in Summer (POLARIS) mission, J. Geophys. Res.-Atmos., 104, 26687–26703, https://doi.org/10.1029/1999JD900246, 1999.

Gu, Y., Liu, B., Li, Y., Zhang, Y., Bi, X., Wu, J., Song, C., Dai, Q., Han, Y., Ren, G., and Feng, Y.: Multi-scale volatile organic compound (VOC) source apportionment in Tianjin, China, using a receptor model coupled with 1-hr resolution data, Environ. Pollut., 265, 115023, https://doi.org/10.1016/j.envpol.2020.115023, 2020.

Han, Y., Huang, X., Wang, C., Zhu, B., and He, L.: Characterizing oxygenated volatile organic compounds and their sources in rural atmospheres in China, J. Environ. Sci., 81, 148–155, https://doi.org/10.1016/j.jes.2019.01.017, 2019.

Hong, Z., Li, M., Wang, H., Xu, L., Hong, Y., Chen, J., Chen, J., Zhang, H., Zhang, Y., Wu, X., Hu, B., and Li, M.: Characteristics of atmospheric volatile organic compounds (VOCs) at a mountainous forest site and two urban sites in the southeast of China, Sci. Total Environ., 657, 1491–1500, https://doi.org/10.1016/j.scitotenv.2018.12.132, 2019.

Huang, X.-F., Wang, C., Zhu, B., Lin, L.-L., and He, L.-Y.: Exploration of sources of OVOCs in various atmospheres in southern China, Environ. Pollut., 249, 831–842, https://doi.org/10.1016/j.envpol.2019.03.106, 2019.

Hui, L., Liu, X., Tan, Q., Feng, M., An, J., Qu, Y., Zhang, Y., and Jiang, M.: Characteristics, source apportionment and contribution of VOCs to ozone formation in Wuhan, Central China, Atmos. Environ., 192, 55–71, https://doi.org/10.1016/j.atmosenv.2018.08.042, 2018.

Kim, S., Kim, S.-Y., Lee, M., Shim, H., Wolfe, G. M., Guenther, A. B., He, A., Hong, Y., and Han, J.: Impact of isoprene and HONO chemistry on ozone and OVOC formation in a semirural South Korean forest, Atmos. Chem. Phys., 15, 4357–4371, https://doi.org/10.5194/acp-15-4357-2015, 2015.

Li, C., Liu, Y., Cheng, B., Zhang, Y., Liu, X., Qu, Y., An, J., Kong, L., Zhang, Y., Zhang, C., Tan, Q., and Feng, M.: A comprehensive investigation on volatile organic compounds (VOCs) in 2018 in Beijing, China: Characteristics, sources and behaviours in response to O_3 formation, Sci. Total Environ., 806, 150247, https://doi.org/10.1016/j.scitotenv.2021.150247, 2022.

Li, J., Zhai, C., Yu, J., Liu, R., Li, Y., Zeng, L., and Xie, S.: Spatiotemporal variations of ambient volatile organic compounds and their sources in Chongqing, a mountainous megacity in China, Sci. Total Environ., 627, 1442–1452, https://doi.org/10.1016/j.scitotenv.2018.02.010, 2018.

Li, K., Wang, X., Li, L., Wang, J., Liu, Y., Cheng, X., Xu, B., Wang, X., Yan, P., Li, S., Geng, C., Yang, W., Azzi, M., and Bai, Z.: Large variability of O_3-precursor relationship during severe ozone polluted period in an industry-driven cluster city (Zibo) of North China Plain, J. Clean Prod., 316, 128252, https://doi.org/10.1016/j.jclepro.2021.128252, 2021.

Li, X., Rohrer, F., Brauers, T., Hofzumahaus, A., Lu, K., Shao, M., Zhang, Y. H., and Wahner, A.: Modeling of HCHO and CHOCHO at a semi-rural site in southern China during the PRIDE-

PRD2006 campaign, Atmos. Chem. Phys., 14, 12291–12305, https://doi.org/10.5194/acp-14-12291-2014, 2014.

Li, Y., Yin, S., Yu, S., Yuan, M., Dong, Z., Zhang, D., Yang, L., and Zhang, R.: Characteristics, source apportionment and health risks of ambient VOCs during high ozone period at an urban site in central plain, China, Chemosphere, 250, 126283, https://doi.org/10.1016/j.chemosphere.2020.126283, 2020.

Liu, Y., Shen, H., Mu, J., Li, H., Chen, T., Yang, J., Jiang, Y., Zhu, Y., Meng, H., Dong, C., Wang, W., and Xue, L.: Formation of peroxyacetyl nitrate (PAN) and its impact on ozone production in the coastal atmosphere of Qingdao, North China, Sci. Total Environ., 778, 146265, https://doi.org/10.1016/j.scitotenv.2021.146265, 2021a.

Liu, Y., Wang, H., Jing, S., Peng, Y., Gao, Y., Yan, R., Wang, Q., Lou, S., Cheng, T., and Huang, C.: Strong regional transport of volatile organic compounds (VOCs) during wintertime in Shanghai megacity of China, Atmos. Environ., 244, 117940, https://doi.org/10.1016/j.atmosenv.2020.117940, 2021b.

Liu, Y., Qiu, P., Xu, K., Li, C., Yin, S., Zhang, Y., Ding, Y., Zhang, C., Wang, Z., Zhai, R., Deng, Y., Yan, F., Zhang, W., Xue, Z., Sun, Y., Ji, D., Li, J., Chen, J., Tian, H., Liu, X., and Zhang, Y.: Analysis of VOC emissions and O_3 control strategies in the Fenhe Plain cities, China, J. Environ. Manage, 325, 116534, https://doi.org/10.1016/j.jenvman.2022.116534, 2023.

Ma, Z., Liu, C., Zhang, C., Liu, P., Ye, C., Xue, C., Zhao, D., Sun, J., Du, Y., Chai, F., and Mu, Y.: The levels, sources and reactivity of volatile organic compounds in a typical urban area of Northeast China, J. Environ. Sci., 79, 121–134, https://doi.org/10.1016/j.jes.2018.11.015, 2019.

Simayi, M., Shi, Y., Xi, Z., Li, J., Yu, X., Liu, H., Tan, Q., Song, D., Zeng, L., Lu, S., and Xie, S.: Understanding the sources and spatiotemporal characteristics of VOCs in the Chengdu Plain, China, through measurement and emission inventory, Sci. Total Environ., 714, 136692, https://doi.org/10.1016/j.scitotenv.2020.136692, 2020.

Song, M., Tan, Q., Feng, M., Qu, Y., Liu, X., An, J., and Zhang, Y.: Source Apportionment and Secondary Transformation of Atmospheric Nonmethane Hydrocarbons in Chengdu, Southwest China, J. Geophys. Res.-Atmos., 123, 9741–9763, https://doi.org/10.1029/2018JD028479, 2018.

Song, M., Li, X., Yang, S., Yu, X., Zhou, S., Yang, Y., Chen, S., Dong, H., Liao, K., Chen, Q., Lu, K., Zhang, N., Cao, J., Zeng, L., and Zhang, Y.: Spatiotemporal variation, sources, and secondary transformation potential of volatile organic compounds in Xi'an, China, Atmos. Chem. Phys., 21, 4939–4958, https://doi.org/10.5194/acp-21-4939-2021, 2021.

Tan, Z., Fuchs, H., Lu, K., Hofzumahaus, A., Bohn, B., Broch, S., Dong, H., Gomm, S., Haeseler, R., He, L., Holland, F., Li, X., Liu, Y., Lu, S., Rohrer, F., Shao, M., Wang, B., Wang, M., Wu, Y., Zeng, L., Zhang, Y., Wahner, A., and Zhang, Y.: Radical chemistry at a rural site (Wangdu) in the North China Plain: observation and model calculations of OH, HO_2 and RO_2 radicals, Atmos. Chem. Phys., 17, 663–690, https://doi.org/10.5194/acp-17-663-2017, 2017.

Tan, Z., Lu, K., Jiang, M., Su, R., Wang, H., Lou, S., Fu, Q., Zhai, C., Tan, Q., Yue, D., Chen, D., Wang, Z., Xie, S., Zeng, L., and Zhang, Y.: Daytime atmospheric oxidation capacity in four Chinese megacities during the photochemically polluted season: a case study based on box model simulation, Atmos. Chem. Phys., 19, 3493–3513, https://doi.org/10.5194/acp-19-3493-2019, 2019.

Wang, N., Li, N., Liu, Z., and Evans, E.: Investigation of chemical reactivity and active components of ambient VOCs in Jinan, China, Air Qual Atmos Health, 9, 785–793, https://doi.org/10.1007/s11869-015-0380-1, 2016.

Wang, X., Yin, S., Zhang, R., Yuan, M., and Ying, Q.: Assessment of summertime O_3 formation and the O_3-NO_x-VOC sensitivity in Zhengzhou, China using an observation-based model, Sci. Total Environ., 813, 152449, https://doi.org/10.1016/j.scitotenv.2021.152449, 2022.

Xu, K., Liu, Y., Li, C., Zhang, C., Liu, X., Li, Q., Xiong, M., Zhang, Y., Yin, S., and Ding, Y.: Enhanced secondary organic aerosol formation during dust episodes by photochemical reactions in the winter in Wuhan, J. Environ. Sci., 133, 70–82, https://doi.org/10.1016/j.jes.2022.04.0181001-0742, 2023.

Xu, Z., Wang, T., Xue, L. K., Louie, P. K. K., Luk, C. W. Y., Gao, J., Wang, S. L., Chai, F. H., and Wang, W. X.: Evaluating the uncertainties of thermal catalytic conversion in measuring atmospheric nitrogen dioxide at four differently polluted sites in China, Atmos. Environ., 76, 221–226, https://doi.org/10.1016/j.atmosenv.2012.09.043, 2013.

Yang, Y., Shao, M., Keßel, S., Li, Y., Lu, K., Lu, S., Williams, J., Zhang, Y., Zeng, L., Nölscher, A. C., Wu, Y., Wang, X., and Zheng, J.: How the OH reactivity affects the ozone production efficiency: case studies in Beijing and Heshan, China, Atmos. Chem. Phys., 17, 7127–7142, https://doi.org/10.5194/acp-17-7127-2017, 2017.

Yang, Y., Wang, Y., Huang, W., Yao, D., Zhao, S., Wang, Y., Ji, D., Zhang, R., and Wang, Y.: Parameterized atmospheric oxidation capacity and speciated OH reactivity over a suburban site in the North China Plain: A comparative study between summer and winter, Sci. Total Environ., 773, 145264, https://doi.org/10.1016/j.scitotenv.2021.145264, 2021.

Zhang, Z., Sun, Y., and Li, J.: Characteristics and sources of VOCs in a coastal city in eastern China and the implications in secondary organic aerosol and O_3 formation, Sci. Total Environ., 887, 164117, https://doi.org/10.1016/j.scitotenv.2023.164117, 2023.